Photoluminescent Enzymatic Sensor Based on Nanoporous Anodic Alumina

5 AUTHORS, INCLUDING:

Abel Santos
University of Adelaide
95 PUBLICATIONS **584** CITATIONS

SEE PROFILE

Josep Ferre-Borrull
Universitat Rovira i Virgili
160 PUBLICATIONS **1,174** CITATIONS

SEE PROFILE

Josep Pallarès
Universitat Rovira i Virgili
213 PUBLICATIONS **2,086** CITATIONS

SEE PROFILE

L. F. Marsal
Universitat Rovira i Virgili
245 PUBLICATIONS **2,204** CITATIONS

SEE PROFILE

# Photoluminescent Enzymatic Sensor Based on Nanoporous Anodic Alumina

Abel Santos, Gerard Macías, Josep Ferré-Borrull, Josep Pallarès, and Lluís F. Marsal*

Departament d'Enginyeria Electrònica, Elèctrica i Automàtica, Universitat Rovira i Virgili, Avenida Països Catalans 26, 43007 Tarragona, Spain

S *Supporting Information*

ABSTRACT: Herein, we present a smart enzymatic sensor based on nanoporous anodic alumina (NAA) and its photoluminescence (PL) in the UV−visible range. The as-produced structure of NAA is functionalized and activated in order to perform the enzyme immobilization in a controlled manner. The whole process is monitored through the PL spectrum and each stage is characterized by an exclusive barcode, which is associated with the PL oscillations. This characteristic property allows us to calculate the change in the effective optical thickness that takes place after each stage. This makes it possible to accurately detect and quantify the immobilized enzyme within the NAA structure. Finally, the NAA geometry (i.e., the pore length and its diameter) is optimized to improve the enzyme immobilization and its detection inside the pores. This enzymatic sensor can give quick and accurate measurements of enzyme levels, what is crucial in clinical enzymology to prevent and detect diseases at their primary stage.

KEYWORDS: *nanoporous alumina, barcodes, enzyme detection, immobilization, biosensor*
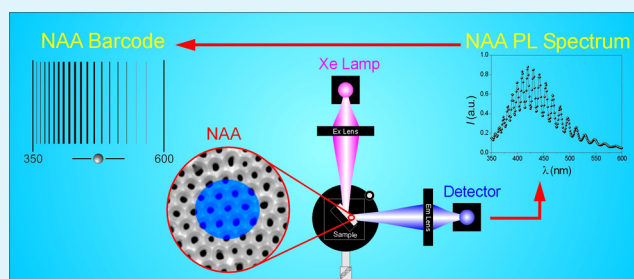
■ INTRODUCTION

Enzymes are proteins that have the main function of catalyzing a wide range of biochemical reactions. Although the first studies about enzymes date back to the late 19th century, humanity has used them for thousands of years in multiple processes (e.g., sugar fermentation to alcohol, breaking down lactose to glucose, hydrolyzation of proteins in cheese manufacture, etc.). Furthermore, enzymes are involved in many reactions that take place in the activity of the human body (e.g., digestion, metabolism, respiration, etc.). High or low levels of them can be a sign of important diseases (e.g., pancreatitis, metabolomic malfunctions, and so forth).[1] For this reason, current clinical enzymology requires improved enzymatic sensors in terms of quickness, sensitivity, selectivity and biocompatibility. Among the diagnostic techniques used in clinical enzymology (e.g., radiometry, potentiometry, conductometry, etc.), photoluminescence (PL) is one of the most suitable for its technical characteristics (i.e., velocity, accuracy, reproducibility, sensitivity, selectivity, and so on).[2,3] Trypsin is a serine protease produced in the pancreas, the function of which is to hydrolyze peptides into amino acids in the digestive system. This makes it possible the absorption of peptides through the small intestine lining.

A low level of trypsin or other digestive enzymes as ptyalin, pepsin, lipase, and protease can be a sign of serious pancreatic diseases as chronic pancreatitis or pancreatitic cancer.[4] Therefore, the correct interpretation of signs and symptoms as well as the availability of reliable biosensors, which give fast and accurate measurements of enzyme levels, are crucial factors to prevent and detect diseases at opportune time (i.e., at their primary stage when they can be controlled by a suitable medical treatment).

Optical biosensors based on porous materials have demonstrated to be outstanding devices for detecting and studying multiple biological substances and processes. These biosensors have been successfully tested in some biological processes.[5−8] For instance, porous silicon colloids with spherical shape have demonstrated to be potential optical biosensors in the near IR region.[9,10] Interferometric sensors based on nanoporous anodic alumina (NAA) are envisaged for detecting binding events of biological molecules as DNA or volatile substances related to diseases as sulfur.[11,12] A basic plasmon resonance spectroscopic sensor based on NAA has been used for establishing the activity of immobilized invertase.[13] More recently, we reported on the development of an optical biosensing barcode system based on the photoluminescence of NAA in the UV−visible region.[14] Likewise in the universal product code (UPC), in that system, each bar position corresponds to the wavelength of each oscillation in the PL spectrum and the higher the oscillation intensity the wider the bar.[15] Thence, a unique barcode is related to the NAA geometry (i.e., the pore length and its diameter) by means of its PL spectrum, which can be structurally tuned at will. This enables the generation of a

wide range of PL barcodes, which are dearly useful for biosensing purposes in the UV−visible region. In our previous work, we demonstrated the biosensing performance of that system to such external biological substances as organic dyes and glucose.

Here, we present a selective enzymatic biosensor based on NAA and its photoluminescence. The basic structure of NAA is functionalized and activated for immobilizing trypsin in a controlled manner. Furthermore, each stage of the process is monitored by the PL spectrum and characterized by an exclusive barcode, what makes it possible to study the whole process by means of the effective optical thickness change. Additionally, the geometric characteristics of NAA (i.e., the pore length and its diameter) are optimized for improving the immobilization and detection of trypsin.

RESULTS AND DISCUSSION

NAA samples are fabricated by the two-step anodization process reported elsewhere (Methods Section).[16] By this method, the pore length (L_p) is controlled by the anodization time (t_{an}) and the pore diameter (d_p) is widened by a wet chemical etching, which is performed after anodizing. To optimize the immobilization and detection processes of trypsin, the pore length and its diameter are each set to three levels (5.3, 6.2, and 7.1 μm and 30, 34, and 39 nm, respectively). So, a total of nine different NAA samples are studied. These samples are labeled as Bio(1−9) and their fabrication conditions and geometric characteristics are summarized in Tables 1S and 2S (Supporting Information), respectively. The smallest pore diameter in the NAA samples is around 30 nm, what is approximately 8-fold larger than the nominal hydrodynamic radius of trypsin (i.e., about 3.8 nm).[17] Therefore, the trypsin molecules can be immobilized on the NAA structure without pore obstruction. Figure 1S in the Supporting Information shows a set of top view scanning electron microscopy (SEM) images of three NAA samples with different pore diameters.

Under certain conditions, the PL spectrum of NAA presents oscillations generated by the Fabry−Pérot effect.[18] This is reflected on an amplification of the PL oscillations due to a strong PL enhancement at wavelengths corresponding to the optical modes of the Fabry−Pérot cavity formed by the system Air−NAA−Aluminum. As a result, the PL spectrum shows an abundance of well-resolved and narrow oscillations, which are dearly useful for sensing purposes. Furthermore, the number, intensity, and position of these oscillations can be adjusted at will by increasing the pore length and its diameter (i.e., by changing the effective medium). The wavelength of each oscillation maximum in the PL spectrum follows the Fabry−Pérot relationship (eq 1)

$$2n_{\mathrm{eff}}L_p = m\lambda \qquad (1)$$

where n_{eff} is the effective refractive index of NAA, L_p is the pore length, and m is the order of the PL oscillation, the maximum of which is located at the wavelength λ.

The product $2n_{\mathrm{eff}}L_p$ is known as the effective optical thickness (OT$_{\mathrm{eff}}$) and can be estimated by calculating the slope of the linear fitting m versus λ^{-1} or by applying the fast Fourier transform to the PL spectrum.

The as-produced NAA samples are tested as enzymatic sensor by measuring the PL spectrum after functionalization, activation and subsequent enzyme immobilization (Methods). This process is divided into several stages (Figure 1). After the
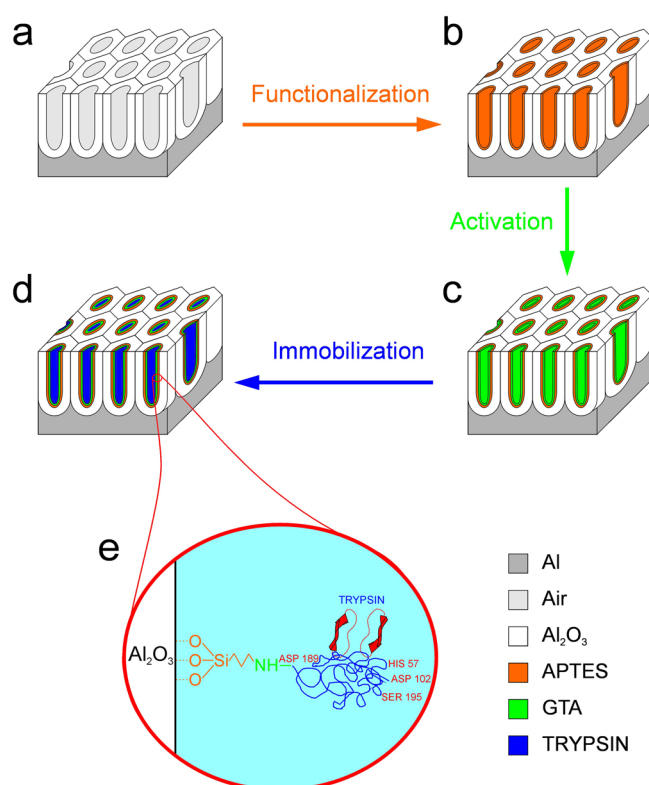
Figure 1. Schematic diagram showing the different stages of the fabrication process of the NAA enzymatic sensor. (a) As-produced NAA. (b) APTES-functionalized NAA. (c) GTA-activated NAA. (d) Trypsin-immobilized NAA. (e) Magnified view of the resulting NAA enzymatic sensor.

fabrication process (i.e., anodization and pore widening) (Figure 1a), as-produced NAA samples are functionalized by silanization with 3-aminopropyltriethoxysilane (APTES) (Figure 1b). Subsequently, the amine group of APTES is activated by incubation in glutaraldehyde (GTA) (Figure 1c). Finally, the immobilization of trypsin is performed by infiltration under controlled conditions to avoid its autolysis (Figure 1d). Because the activated amine group on the pore surface of NAA binds the Asp 189 region of trypsin, the catalytic triad His 57−Asp 102−Ser 195 remains unblocked for cleaving the peptide bonds C-terminal to Arg or Lys residues.[19] Accordingly, the resulting NAA enzymatic sensor could be used as a nanoreactor for protein digestion in multiple industrial applications.[20] For instance, it is known that trypsin obtained from cold-adapted fishes has a high activity at low temperatures. This is a very interesting property for several industrial applications, such as in certain food processing operations that require low processing temperatures.[21]

Each stage of this process implies a modification of the effective refractive index and thus a change in the effective optical thickness. This enables the characterization of these stages by a specific barcode and an exclusive value of OT$_{\mathrm{eff}}$, which is obtained from the PL spectrum (Figure 2). Therefore, we are able to qualitatively detect the immobilized enzymes by means of the increment in the effective optical thickness (ΔOT$_{\mathrm{eff}}$). Figure 3a summarizes the values of the effective optical thickness increment of a NAA sample measured at the end of each stage. Once the NAA is functionalized, ΔOT$_{\mathrm{eff}}$ increases around 0.6%, what corresponds to the APTES layer that covers the inner surface of the pores. The activation of
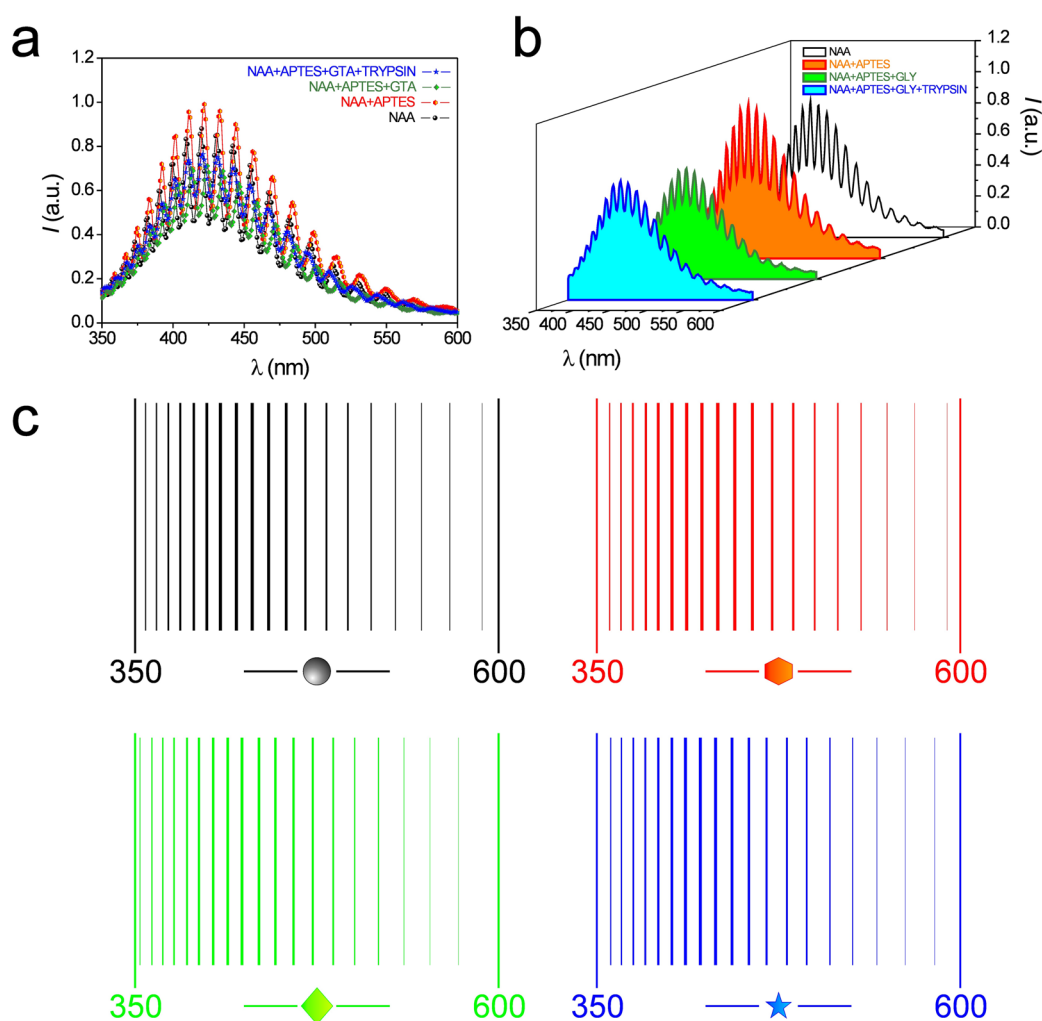
Figure 2. Photoluminescence spectra of sample Bio (1) as a function of the fabrication stage and resulting barcodes after encoding these PL spectra (λ_{ex} = 320 nm). (a) Overlapped PL spectra, (b) 3D PL spectra, (c) resulting barcodes obtained after coding these spectra.

APTES with GTA produces an additional 1.2% increment of ΔOT_{eff}. Finally, after immobilizing trypsin in the NAA structure, there is an extra 1.8% increase in ΔOT_{eff}.

Additionally, all the process is analyzed by Fourier transform infrared (FTIR) (see Figure 2S in the Supporting Information). The different functional groups on the NAA surface created after each stage of the fabrication process are identified by the absorption bands in the FTIR spectrum.

Finally, to optimize the enzymatic sensor performance, the geometric characteristics of NAA (i.e., the pore length and its diameters) are slightly modified. Table 3S in the Supporting Information compiles the values of the effective optical thickness increment of all these NAA samples measured at the end of each stage. Furthermore, Figure 3b shows the contour plot of ΔOT_{eff} as a function of L_p and d_p for all the samples during the immobilization stage, which is the most interesting from the enzymatic sensitivity point of view. As for this, it is demonstrated that the highest relative change of the effective optical thickness increment takes place for the NAA sample fabricated at an anodization time of 90 min and a pore widening of 2.5 min. In other words, the pore geometry L_p = 5.3 μm and d_p = 34 nm is envisaged for developing the most optimum enzymatic sensor, because it presents the highest sensitivity to trypsin.

As was commented above, some optical porous nanostructures have been successfully used as a base for developing similar optical biosensors.[10,22−25] Nonetheless, the proposed enzymatic sensor based on NAA has some advantages for studying enzymatic events:

(A) This barcode system opens a new window toward automatic, objective, accurate and fast measurements of enzyme levels. This system yields a huge number of different barcodes for producing exclusive spectroscopic signatures in the UV−visible region, which is of extreme importance to perform fast and precise diagnostics in clinical enzymology.

(B) The NAA geometry can be accurately controlled by the fabrication parameters. Hence, the pore geometry can be adjusted to enable the target molecule immobilization along large pores. The sensing ability of such techniques as surface plasmon resonance has a remarkable worsening as the pore length increases.[7,9] Contrarily, the PL spectrum can be tuned ad lib in the UV−visible region for a wide range of pore lengths (i.e., from 5 to 12 μm, approximately).[14]

(C) In contrast to other materials such as porous silicon, the PL spectrum of NAA is practically stable throughout and it is not necessary to passivate NAA to avoid shifts in the oscillation positions.[10,26] This guarantees that the performed measurements are reliable and reproducible.
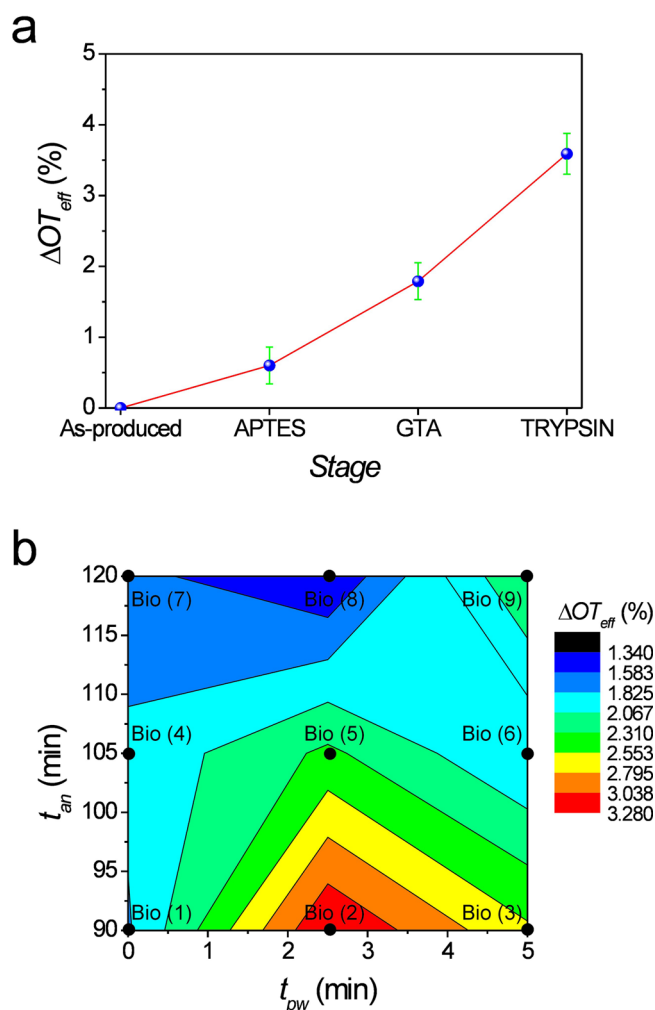
Figure 3. Change in the effective optical thickness increment as a result of the different fabrication stages. (a) ΔOT_{eff} at each fabrication stage of sample Bio (1). (b) Contour graph of ΔOT_{eff} as a function of the anodization time (t_{an}) and pore widening time (t_{pw}) for samples Bio(1−9).

(D) The pores in NAA have a well-defined cylindrical geometry with smooth walls. This enables their functionalization with many functional substances (e.g., silanes, oxides, proteins, polymers, etc.).[11,27] Moreover, by means of this, the surface chemistry of NAA can be changed ad libitum for endowing NAA with a high selectivity to multiple target molecules (e.g., DNA, antibodies, enzymes, lipids, and so forth).

(E) From the industrial point of view, the immobilized enzymes are more suitable than free enzymes because this technique makes it possible to recycle the enzymatic reactors for several reaction cycles and their properties (e.g., activity, stability and selectivity) are noticeably improved.[28] Furthermore, an additional washing stage after the digestive process could extend the enzymatic reactor use for multiple cycles.

(F) The physical properties of NAA (e.g., biocompatibility, thermal stability, environmental resistance, controlled photoluminescence, etc.) combined with its versatile geometry (i.e., wide range of pore length and diameter) make NAA an excellent material for biotechnological applications.

(G) Photoluminescence is considered more suitable than photometry and radioimmunoassay for studying the reactions between enzymes and their specific substrates because these are commonly labeled with photoluminescent dyes (e.g., Z-Gly-Gly-Arg-7-amido-4-methylcoumarin).[2,3]

CONCLUSIONS

To conclude, we have proposed a smart enzymatic sensor based on the photoluminescence of nanoporous anodic alumina in the UV−visible range. This sensor is developed from as-produced NAA in several stages (i.e., functionalization, activation and enzyme immobilization). These stages are characterized by measuring the effective optical thickness change obtained from the PL spectrum. Additionally, the sensitivity of this enzymatic sensor is tested and optimized as a function of the pore geometry. This optical biosensor can be integrated with an objective and systematic barcode system, what coverts NAA into an outstanding candidate for developing a new generation of clinical enzymatic sensors or industrial enzymatic nanoreactors.

METHODS

NAA Fabrication. NAA samples were produced by the two-step anodization procedure.[16] Commercial aluminum (Al) foils were electropolished in a mixture of ethanol (EtOH) and perchloric acid ($HClO_4$) 4:1 (v:v) at 20 V for 4 min. Subsequently, the first anodization step was carried out in an aqueous solution of oxalic acid ($H_2C_2O_4$) 0.3 M at 40 V and 5 °C for 20 h. The alumina layer with disordered pores was then selectively dissolved by wet chemical etching in a mixture of phosphoric acid (H_3PO_4) 0.4 M and chromic acid (H_2CrO_7) 0.2 M at 70 °C. Afterward, the second anodization step was performed under the same anodization conditions as the first step. Depending on the NAA sample, the anodization time during this step was adjusted to modify the pore length (i.e., 90, 105, and 120 min). Finally, the pore diameter was widened by a wet chemical etching in an aqueous solution of H_3PO_4 5 wt %.

NAA Characterization. NAA samples were characterized by scanning electron microscopy (SEM FEI Quanta 600). The photoluminescence measurements were obtained from a fluorescence spectrophotometer from Photon Technology International Inc. with a Xe lamp used as the excitation light source at room temperature and an excitation wavelength (λ_{ex}) of 320 nm. The FTIR measurements were carried out in a FTIR spectrometer Bruker Vertex 70 equipped with a Tungsten (W) and Globar sources for the NIR-MIR range. The standard image processing package (ImageJ, public domain program developed at the RSB of the NIH, USA) was used to perform the SEM image analysis.[29]

Enzymatic Sensor Fabrication. First, as-produced NAA samples were hydroxylated by immersion in hydrogen peroxide (H_2O_2) 30 wt % for 45 min at 70 °C and slightly dried under a nitrogen (N_2) stream. Then, hydroxylated NAA samples were functionalized in a solution of 3-aminopropyltriethoxysilane (APTES) 5 v% diluted in acetone (C_3H_6O) for 2 h at room temperature. Subsequently, to cross-link the silane molecules, functionalized NAA samples were washed in acetone and cured for 2 h at 110 °C under air atmosphere. After this, the amine group of APTES was activated by incubation in a phosphate buffer solution (PBS) of glutaraldehyde (GTA) 2.5 v% at pH 7.4 and room temperature. Finally, after washing these activated NAA samples with PBS, the trypsin immobilization was conducted by dipping these activated NAA samples into a PBS solution of trypsin 0.1 mg mL^{-1} for 4 h at 4 °C and pH 7.4. The autolysis of trypsin was restricted by adding 50 mM benzamidine ($C_7H_8N_2$) to the trypsin solution. The unimmobilized trypsin was removed by washing the samples with PBS and the residual aldehyde groups were depleted by a solution of tris(hydroxymethyl)aminomethane hydrochloride (Tris-HCl) 1 M at adjusted pH 7.4. To guarantee the sensor response reproducibility, we repeated all the experiments three times, and the obtained results were statistically treated.

3587

dx.doi.org/10.1021/am300648j | ACS Appl. Mater. Interfaces 2012, 4, 3584−3588

■ ASSOCIATED CONTENT

Ⓢ Supporting Information

Additional images and tables (PDF). This material is available free of charge via the Internet at http://pubs.acs.org.

■ AUTHOR INFORMATION

Corresponding Author

*E-mail: lluis.marsal@urv.cat. Tel.: +34 977559625. Fax: +34 977 559605.

Notes

The authors declare no competing financial interest.

■ ACKNOWLEDGMENTS

■ REFERENCES

(1) Maté, J. M.; Pérez-Gómez, C.; Núñez de Castro, I. *Clin. Biochem.* **1999**, *32*, 595−603.

(2) Pearson, K. W.; Smith, R. E.; Mitchell, A. R.; Bissel, E. R. *Clin. Chem.* **1961**, *27*, 256−262.

(3) Smith, R. E. *J. Histochem. Cytochem.* **1984**, *32*, 1265−1274.

(4) Fedail, S. S.; Harvey, R. F.; Salmon, P. R.; Brown, P.; Read, A. E. *Gut* **1979**, *20*, 983−986.

(5) Szili, E. J.; Jane, A.; Low, S. P.; Sweetman, M.; Macardle, P.; Kumar, S.; Smart, R. St. C.; Voelcker, N. H. *Sens. Actuators, B* **2011**, *160*, 341−348.

(6) DeLouise, L. A.; Miller, B. L. *Anal. Chem.* **2005**, *77*, 1950−1956.

(7) DeLouise, L. A.; Kou, P. M.; Miller, B. L. *Anal. Chem.* **2005**, *77*, 3222−3230.

(8) Dronov, R.; Jane, A.; Shapter, J. G.; Hodges, A.; Voelcker, N. H. *Nanoscale* **2011**, *3*, 3109−3114.

(9) Fenollosa, R.; Ramiro-Manzano, F.; Tymczenko, M.; Meseguer, F. *J. Mater. Chem.* **2010**, *20*, 5210−5214.

(10) Ramiro-Manzano, F.; Fenollosa, R.; Xifré-Pérez, E.; Garín, M.; Meseguer, F. *Adv. Mater.* **2011**, *23*, 3022−3025.

(11) Alvarez, S. D.; Li, C. P.; Chiang, C. E.; Schuller, I. K.; Sailor, M. J. *ACS Nano* **2009**, *10*, 3301−3307.

(12) Kumeria, T.; Parkinson, L.; Losic, D. *Nanoscale Res. Lett.* **2011**, *6*, 634.

(13) Dhathathreyan, A. *J. Phys. Chem. B* **2011**, *115*, 6678−6682.

(14) Santos, A.; Balderrama, V. S.; Alba, M.; Formentín, P.; Ferré-Borrull, J.; Pallarès, J.; Marsal, L. F. *Adv. Mater.* **2012**, *24*, 1050−1054.

(15) Palmer, R. C. *The Bar Code Book: Reading, Printing, and Specification of Bar Code Symbols*, 5th ed.; Tafford Publishing: Bloomington, IN, 2007.

(16) Masuda, H.; Fukuda, K. *Science* **1995**, *268*, 1466−1468.

(17) Min, Q.; Wu, R.; Zhao, L.; Qin, H.; Ye, M.; Zhu, J. J.; Zou, H. *Chem. Commun.* **2010**, *46*, 6144−6146.

(18) Huang, K.; Pu, L.; Shi, Y.; Han, P.; Zhang, R.; Zheng, Y. D. *Appl. Phys. Lett.* **2006**, *89*, 201118.

(19) Northrop, J. H.; Kunitz. *Science* **1931**, *73*, 262−263.

(20) Bernd, W.; Darder, M.; Aranda, P.; Ruiz-Hitzky, E. *ACS Appl. Mater. Interfaces* **2011**, *3*, 4339−4348.

(21) Fuchise, T.; Sekizaki, H.; Kishimura, H.; Klomklao, S.; Nalinanon, S.; Benjakul, S.; Chun, B. S. *J. Amino Acids* **2011**, 912382.

(22) Cunin, F.; Schmedake, T. A.; Link, J. R.; Li, Y. Y.; Koh, J.; Bhatia, S. N.; Sailor, M. J. *Nat. Mater.* **2002**, *1*, 39−41.

(23) Chiappini, C.; Liu, X.; Fakhoury, J. R.; Ferrari, M. *Adv. Funct. Mater.* **2010**, *20*, 2231−2239.

(24) Meade, S. O.; Sailor, M. J. *Phys. Status Solidi RRL* **2007**, *1*, R71−R73.

(25) He, B.; Son, S. J.; Lee, S. B. *Anal. Chem.* **2007**, *79*, 5257−5263.

(26) Canham, L. T.; Reeves, C. L.; Newey, J. P.; Houlton, M. R.; Cox, T. I.; Buriak, J. M.; Stewart, M. P. *Adv. Mater.* **1999**, *11*, 1505−1507.

(27) Md Jani, A. M.; Kempson, I. M.; Losic, D.; Voelcker, N. H. *Angew. Chem., Int. Ed.* **2010**, *49*, 7933−7937.

(28) Guisan, J. M. *Immobilization of Enzymes and Cells*; Humana Press: Totowa, NJ, 2006.

(29) Abràmoff, M. D.; Magalhaes, P. J.; Ram, S. J. *Biophotonics Int.* **2004**, *11*, 36−42.